THE EVALUATION OF AMMONIA/HYDROGEN COMBUSTION ON THE H PERMEATION AND EMBRITTLEMENT OF NICKEL-BASE SUPERALLOYS

Marina Kovaleva
College of Physical Sciences and Engineering, Cardiff University, Queen's Building, Cardiff, CF24 3AA, UK

Dominik Dziedzic
Department of Mechanical Engineering, University College London, Roberts Building, Torrington Place, London, WC1E 7JE, UK

Syed Mashruk
College of Physical Sciences and Engineering, Cardiff University, Queen's Building, Cardiff CF24 3AA, UK

Sam Evans
College of Physical Sciences and Engineering, Cardiff University, Queen's Building, Cardiff, CF24 3AA, UK

Agustin Valera-Medina
College of Physical Sciences and Engineering, Cardiff University, Queen's Building, Cardiff, CF24 3AA, UK

Enrique Galindo-Nava
Department of Mechanical Engineering, University College London, Roberts Building, Torrington Place, London, WC1E 7JE, UK

ABSTRACT

Recent studies exploring ammonia as a green hydrogen energy carrier have established its suitability for a variety of combustion technologies including gas turbines, furnaces, and internal combustion engines. Of significant interest are ammonia/hydrogen blends, which possess combustion benefits over pure ammonia, including an extended stability range and higher laminar burning velocity. Despite the extensive research to characterise the flame properties of these blends, very few studies explore the suitability of existing materials for the manufacture of ammonia/hydrogen combustors. The present study evaluates the impact of ammonia/hydrogen flame chemistry on the H permeation and possible loss of ductility of nickel-superalloys through exposing the samples to pure methane and ammonia/hydrogen flames at atmospheric pressure for a 5-hour period. The effect of the two flame compositions on the materials are compared through thermal desorption analysis (TDA) and room temperature tensile testing. The results showed that exposure to ammonia/hydrogen combustion environments led to hydrogen being absorbed by the nickel superalloys but a possible variation in ductility is influenced by the combustion conditions. Furthermore, the formation of an oxide layer was shown to likely impact the hydrogen absorption rate of the materials. This work shows that ammonia/hydrogen flame chemistry on combustor materials should not be ignored and warrants further studies on material's mechanical and environmental stability controlled by nitrogen and hydrogen species permeating at industrially relevant conditions.

Keywords: Ammonia/hydrogen fuel, nickel superalloys, metal corrosion, H absorption

1. INTRODUCTION

Since the start of the 20th century and the development of the Haber Bosch process, ammonia has not only revolutionised agricultural sector as a cheap and readily available fertiliser but has also gathered interest as a fuel. Examples include Belgium's adaption of around 100 buses to run on an ammonia/coal gas blends during the World War II diesel shortages [1] and NASA's development of the X-15 hypersonic powered aircraft powered by anhydrous ammonia [1]. Many lessons can also be learnt from the efforts of the US Army in the 1960s to develop ammonia gas turbines and internal combustion engines [2-4], though the projects did not progress further due to low combustion efficiency. However, in recent years, fuel ammonia has gained even more attention as a convenient and affordable hydrogen energy carrier to tackle global warming. This has led to a variety of demonstration projects [5] and detailed studies on the combustion properties of this fuel [6].

These studies have shown that pure ammonia powered devices are susceptible to having a low range of stability and low laminar burning velocity, compared to traditional fossil fuel options. Hence the focus of ammonia-fuelled devices has shifted to ammonia blends containing fuels of higher reactivity such as methane or hydrogen. While ammonia/methane blends may be more important in the short-term adaption of existing fossil-fuel devices, ammonia/hydrogen blends are more relevant achieving

longer term, net-zero targets, providing the motivation to use an ammonia/hydrogen blend in the present study.

This work aims to compare the effects metals exposed to two types of flame: a pure methane flame of equivalence ratio, $\varphi = 0.65$ and a 30%/70% (vol.) hydrogen/ammonia flame of equivalence ratio $\varphi = 1.20$. The rationale for selecting this methane equivalence ratios is to use a condition comparable to lean premixed combustion (LPC), an established method employed in dry low emissions (DLE) stationary gas turbines run on natural gas [7-8]. On the other hand, a rich equivalence ratio is often selected by ammonia/hydrogen combustion studies to decrease NOx, and as a step towards a rich-quench-lean (RQL) combustor configuration [9].

Radical quenching of metal wall surfaces has been shown to have an impact on flame properties through the mass transfer of radicals between the flame and wall [16]. However, at time of writing, there is little data to describe this behaviour for ammonia-based fuels. Most studies focus on the behaviour of pure methane [17] or hydrogen flames [18], or otherwise describe the catalysis of pure ammonia decomposition on surfaces [19]. Therefore, there are few (if any) detailed reaction mechanisms that can model this behaviour to aid understanding of the impact of materials on both combustion characteristics and on material properties.

However, previous studies have explored various ammonia-based combustion blends on the properties of metals. Starostin et al. [10] exposed stainless steels and nickel superalloys to a solution of highly concentrated aqueous ammonium nitrate/urea solution, to understand corrosion effects of high nitrogen content fuels. This work suggests that alloys with high Cr (>23% wt.) have good performance in ammonia-based combustion environments, due to the formation of a protective chromium-rich oxide layer. Of further interest is that at high exposure times of 200 hours and high pressures (20MPa), it was possible to differentiate between the impact of the turbulent hot reactor zone (HRZ) at around 745°C and the laminar cold reactor zone (CRZ) at 545°C on stainless steel samples [11]. However, such studies have not been conducted for ammonia/hydrogen flames.

Aside from high temperature corrosion, hydrogen embrittlement is another potential concern in the use of rich ammonia/hydrogen blends. Studies involving hydrogen charging through cathodic hydrogen polarisation at slightly elevated temperatures are widely used to understand the effects of hydrogen on metals. Results focused on superalloy Inconel 718 showed that when compared to samples that were only solution annealed, those that also received additional heat treatment (creating aged and over-aged conditions) had higher levels of embrittlement due to the precipitation of γ', γ'' phases. Furthermore, the solution annealed condition specimens presented an increase in strength due to hydrogen exposure, although these specimens also had higher levels of hydrogen diffusion and permeation than the aged or over-aged conditions [12], also discussed in other studies of nickel superalloys [13-14]. Consequently, understanding how hydrogen concentration changes with microstructure, i.e. γ', γ'' and δ phases, are important for evaluation of candidate materials for ammonia/hydrogen combustors.

Therefore, this work aims to quantify the effects of ammonia/hydrogen flame chemistry on nickel superalloys in comparison traditional methane flame chemistry. Specifically, H concentration inside alloys is measured through thermal desorption analysis (TDA). Tensile tests of materials exposed to both flames are also conducted on three nickel-based alloys to study possible loss of ductility induced by hydrogen embrittlement. The present work serves as enabling methodology for the understanding of surface chemistry, environmental degradation, and development of high temperature materials in ammonia/hydrogen combustion systems.

2. MATERIALS AND METHODS

2.1 Combustion Setup

Figure 1 shows the schematic for the exposure of the metal samples to ammonia/hydrogen flames. However, for the methane flame condition, the ammonia inlet was replaced with methane and the hydrogen inlet was blocked.

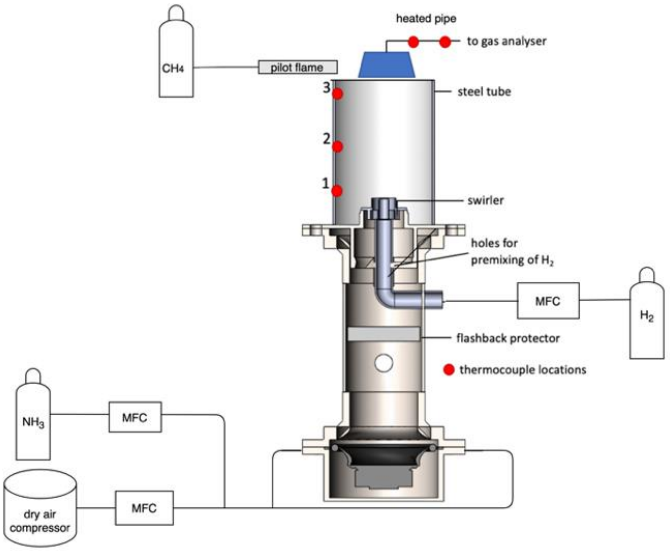

FIGURE 1: SCHEMATIC OF COMBUSTION SETUP

A blend of hydrogen/ammonia at equivalence ratio, ϕ=1.20 was selected for the ammonia-based flame and a pure methane flame of equivalence ratio ϕ=0.65 was used for comparison, with both flames at 5 kW power. The hydrogen fuel fraction was set at X_{H2}=30% for the hydrogen/ammonia flame, as defined in Equation 1:

$$X_{H2} = \frac{[H_2]}{[H_2]+[NH_3]} \cdot 100\% \qquad (1)$$

Where $[H_2]$ and $[NH_3]$ mark the mole fraction of hydrogen and ammonia respectively. The combustion rig featured a fully

premixed swirl burner, with hydrogen mixing holes in the hydrogen inlet pipe to achieve this effect. The flame was enclosed in a stainless-steel sleeve with the following dimensions: 300mm height, 82 mm inner diameter, 4mm wall thickness.

All alloys, provided by Special Metals Wiggin, were suppled in solution annealed condition in sheet form, specific to aerospace applications. The materials tested in the present study and their alloy composition are listed in Table 1.

TABLE 1: COMPOSITIONS OF NICKEL-BASED ALLOYS

	Inconel 617	**Inconel 740H**	**Inconel N06230**	**Inconel HX**
Al	0.8-1.5	0.2-2.0	0.20-0.50	-
B	0.006 max.	0.006 max.	0.015 max.	-
C	0.05-0.15	0.005-0.08	0.05-0.15	0.05-0.15
Co	10.0-15.0	15.0-20.0	5.0 max.	0.5-2.5
Cu		0.05 max.	-	-
Cr	20.0-24.0	23.5-25.5	20.0-24.0	20.5-23.0
Fe	3.0 max.	3.0 max.	3.0 max.	17.0-20.0
La	-	-	0.005-0.050	-
Mn	1.0 max	1.0 max.	0.30-1.00	1.0 max.
Mo	8.0-10.0	2.0 max.	1.0-3.0	8.0-10.0
Nb	-	0.5-2.5	-	-
Ni	44.5	Bal.	Bal.	Bal.
P	-	0.03 max.	0.030 max.	0.04 max.
S	-	0.03 max.	0.015 max.	-
Si	1.0 max	1.0 max.	0.25-0.75	1.0 max.
Ti	0.6 max	0.5-2.5	-	-
W	-	-	13.0-15.0	0.2-1.0

Both combustion runs featured a 10-minute methane ignition at the start of the test, where the 5-hour exposure time of the metals was measured from the point at which the flame had stabilized to the required flame condition. Once the test was complete, the samples were cooled for 30 minutes by a room temperature air flow. The samples were immediately placed in small plastic bags and then submerged into Liquid Nitrogen (LN) to prevent H desorption before the next test.

The samples for thermal desorption analysis tests were cut into square flat samples (20mm wall length), while samples for tensile testing were cut following the BS-EN-2032-001 standard [20]. Both types of samples were mounted on hooks at the combustor edge (Fig. 2). In the present work, the temperature profile was measured along the wall of the combustor. To minimize disruption to the flame, near wall temperatures were measured from 883K to 558K and from 743K, to 351K for ammonia/hydrogen and methane flames respectively, with the decreasing temperature along the wall of the combustor corresponding to heat loss along the combustor length.

a)

b)

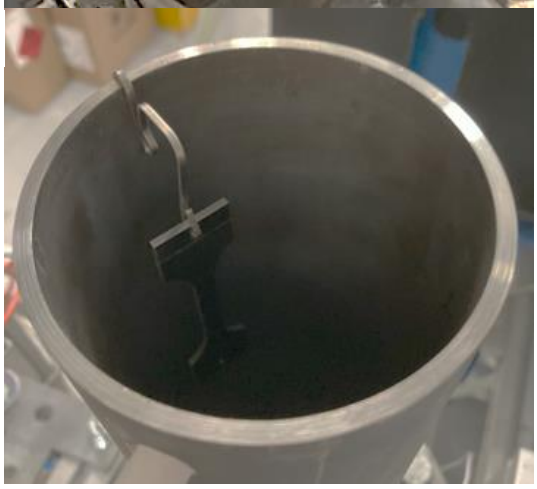

FIGURE 2: THERMOCOUPLE POSITION (A); SAMPLE MOUNTING (B)

There are many barriers to experimentally defining the surface conditions of the samples. The true surface temperature of thin metal samples mounted near the flame zone is difficult to measure with traditional methods such as thermocouples. Gas sampling is an intrusive method that is rarely designed to capture key information for this study, such as concentrations of O, H and OH radicals. Laser diagnostic methods are available for such investigation but are time-intensive and not suitable for a broad comparison of species across the two flame conditions. To counter these challenges, a numerical simulation was conducted, providing an estimated comparison of exposure conditions.

A RANS (Reynolds Averaged Navier Stokes) computational fluid dynamics simulation was carried out following identical geometry, meshing and physics model previously validated for the current experimental rig [21]. For the kinetic reaction mechanism, the reduced mechanism of Gotama et al. [22] and the reduced mechanism of Okafor et al. [23] were used. Thermocouple wall temperatures were used as constant wall temperature inputs in the numerical model, though no additional heat loss or radiation model was used. The

difference in chemical composition (wet values) between the flames is described in Table 2 taken over the distance where each type of sample was mounted.

TABLE 2: FLAME CONDITIONS TAKEN ACROSS SAMPLE MOUNTING POINTS ACCORDING TO THE NUMERICAL SIMULATION

	CH_4 (TDA Sample)	**CH_4 (Tensile Sample)**	**NH_3/H_2 (TDA Sample)**	**NH_3/H_2 (Tensile Sample)**
Temperature (K)	1334-1775	1675-1918	1373-2010	1366-1568
H radical (mol., ppm)	0-7	12-21	57-473	11-57
O radical (mol, ppm)	2-9	18-47	>1	>1
O_2 (mol)	0.010-0.014	0.013-0.019	0	>0.001
H_2 (mol)	0.004 max.	0.004 max.	0.057-0.06	0.052-0.055
N_2 (mol)	0.69	0.69	0.64	0.64
H_2O (mol)	0.25	0.24-0.25	0.30	0.30
NH_3 (mol, %)	>0.01	0	500-3500	3900-5100

Table 2 suggests higher hydrogen concentrations upstream of the combustor, with ammonia/hydrogen flames displaying some unburnt ammonia downstream of the combustor. However, due to the low concentrations of O and O_2 relative to other species, any oxidation on the surface is more likely to be from the air cooling of the samples after the combustion test or from pre-existing oxide scale present on the surface of the alloys. Comparatively, methane flames exhibited oxygen concentration of a few orders of magnitude higher than in the ammonia/hydrogen flame. It was also noted that the location where the TDA samples were mounted were near the flame zone, corresponding to a region where the H radical concentration increases significantly.

2.2 Thermal Desorption Analysis

Thermal desorption analysis (TDA) was performed on the square samples in an Agilent 7890B rig using He as a carrier gas. Two test samples of Inconel HX (corresponding to each flame condition) were removed from the LN and cut in half. One half of each sample had the surface oxide layer removed by grinding the down with a 1200 grit before the cleaning. Samples were ultrasonically cleaned for 5 minutes in ethanol, then washed with isopropanol. After cleaning, the samples ware dried for 4 minutes in a vacuum to remove all hydrocarbons. Samples were then transferred to the thermal desorption rig furnace, which underwent a purging cycle of ~30 min before the start of the desorption experiment. During this time, very little hydrogen was expected to effuse as the diffusivity of H in Ni at room temperature is very low. After the first heating cycle, the sample was held for 4h under 800°C. Following the first run, each sample was subject to the same preparation procedure and during a second TDA test, assuming that all H has left the sample to identify the background noise produced by the machine. All samples followed the same preparation process. The obtained curves were subtracted from the first tests to obtain the real H desorption behaviour.

2.3 Mechanical Testing

Within 15 minutes of being removed from the liquid nitrogen, the tensile samples were tested with a Zwick Z-100 tensile testing machine at a 1mm/min crosshead speed. The percentage elongation across the gauge length was measured as a ratio of the original length to the length after fracture. The measurement was conducted by marking lengths along the sample gauge length and comparing the before and after percentage change and averaging the values. The tensile test samples were prepared and followed dimensions stated in the aerospace standard BS-EN-2032-001 [20].

3. RESULTS AND DISCUSSION

3.1 Material Oxidation

Samples exposed to both flames showed minor surface oxidation (Fig. 3). A possible reason could be due to air introduction during cooling after the combustion tests, however, the temperatures and times involved would be too mild to induce significant oxidation; nonetheless, this warrants further attention in future test procedures. The oxides are of slightly different colouring, suggesting that the oxidation process could evolve differently between materials exposed to flames rich in methane and ammonia/hydrogen.

This is consistent with previous findings on Ni oxide reduction process using hydrogen and methane showing vastly different reduction rates [29]. Aside from nickel oxide, studies have shown [24], [32], that chromium oxide reactions with steam affect oxidation rates of nickel superalloys. The reason is due to the relative increase in steam concentration for the ammonia/hydrogen flames compared to methane flames. In addition, the presence of C in methane and N in ammonia could affect how the oxidation process takes place at the gas/metal interface [30]. Another reason may be due to ammonia/hydrogen tests being conducted under fuel-rich conditions while methane tests being conducted in fuel-lean conditions. As shown in Table 2, the methane flame would have contained a higher oxygen concentration compared to the ammonia/hydrogen flame. However, more experimental, and theoretical work is needed to study these phenomena in detail.

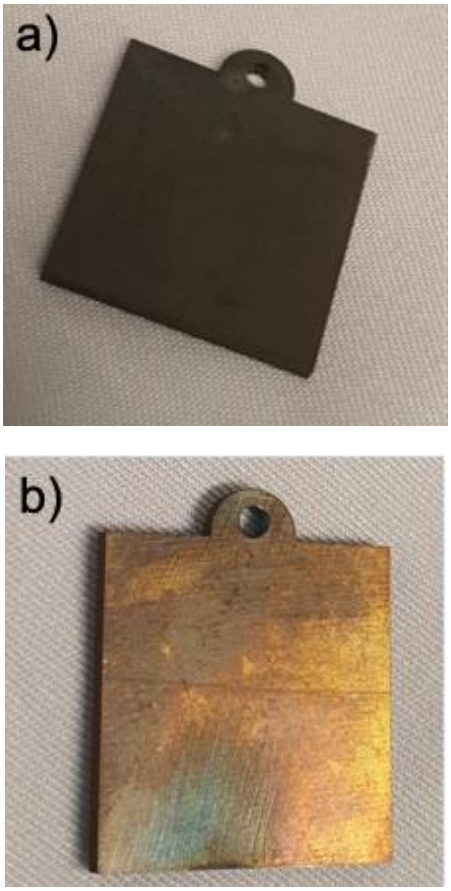

FIGURE 3: INCONEL HX SAMPLES EXPOSED TO A) AMMONIA/HYDROGEN AND B) METHANE

3.2 Thermal Desorption Analysis

Figures 4 and Figure 5 show the TDA results of Inconel HX at a heating rate of 100 ºC/h with and without the removal of the surface oxide layer. The curves for the ammonia/hydrogen flames have a large primary peak at ~400 ºC, a secondary peak at ~550 ºC and a tertiary peak ~ 680ºC. The first peak is indicative of H diffusion and/or weak trapping within the bulk [25], confirming that indeed H permeates under the present (mild) combustion conditions without the need of high pressure, e.g. as in the case of room-temperature gas charging [26]. The second peak could be due to deep trapping taking from pre-existing carbides, whereas the tertiary peak could be connected to remanent oxides. The total hydrogen released from the sample up to 800°C was 1 ppm.

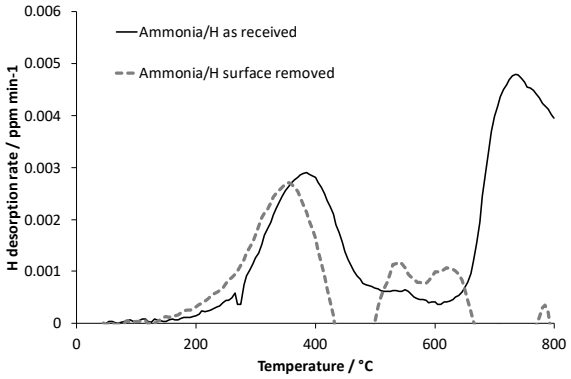

FIGURE 4: TDA RESULTS FOR SAMPLES EXPOSED TO AMMONIA/HYDROGEN

Results for the sample exposed to methane flames are depicted in Fig. 5 showing very little H across all temperatures; this indicates that there is no appreciable diffusible/weakly trapped H and possibly deep trapping in this condition.

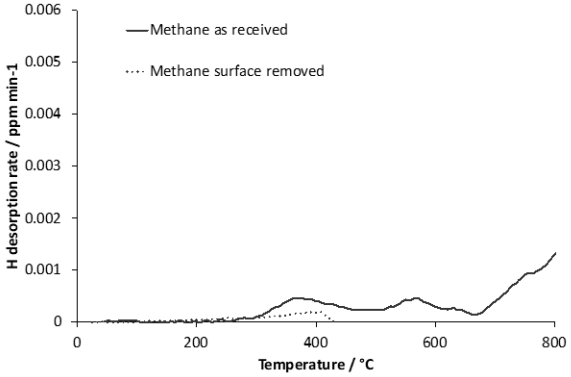

FIGURE 5: TDA RESULTS FOR SAMPLES EXPOSED TO METHANE

To assess the impact of the oxide layer on H permeability and diffusivity, Figure 4 shows additional TDA results for the sample exposed to ammonia/hydrogen flame without removing the oxide layer. The primary peak at ~400ºC remains virtually identical, indicating that the same content of diffusible/weakly trapped H is retained, but it is evident that the hydrogen diffusion behaviour changes drastically at higher temperatures. The secondary peak becomes higher and wider, whereas the tertiary peak drops to very low values and shifts to ~780ºC. The total H content in this sample is 0.42ppm, indicating that oxide layer trapped ~0.58ppm of H. This result confirms that the tertiary peak is most likely driven by the presence of the surface oxide and it acts as a deep trap. However, the present tests are not enough evidence to conclude whether the oxide layer could impact H permeability during the combustion process as it is currently unknown if the oxide forms during/before H permeation occurs or after the H has permeated to the sample.

Nonetheless, the results pave the way towards assessing how ammonia/H flames could change not only material's susceptibility to hydrogen embrittlement but also their oxidation and/or corrosion behaviour.

3.2 Tensile Testing

Figure 6 shows an example stress-strain graph from which UTS and yield stress values were extracted. However, elongation measurements were taken separately and not based on the strain values given in the graphs.

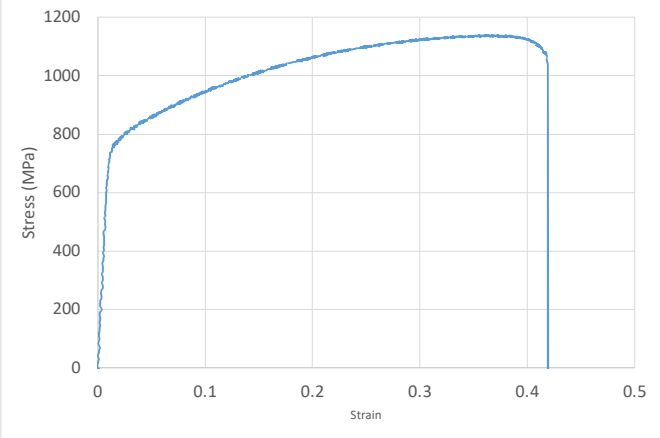

FIGURE 6: INCONEL 740H STRESS-STRAIN GRAPH FOR AMMONIA/HYDROGEN FLAME EXPOSED SAMPLE

Between 6 to 8 samples of each material were tested (giving between 3 to 4 samples each type of flame type), such that Figure 8 shows the averaged ultimate tensile strength across each set of samples, with the error bar taken as the standard deviation of repeat samples.

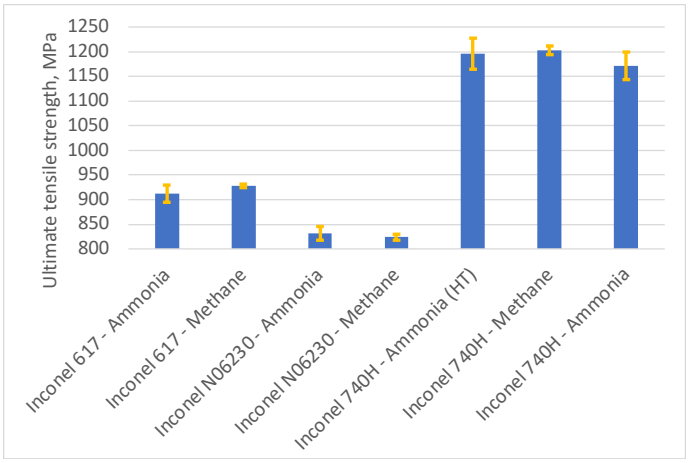

FIGURE 7: UTS VALUES FOR INCONEL 617, INCONEL 740H and INCONEL N06230

Figure 7 suggests that the highest ultimate tensile strength was given by Inconel 740H, with the most variation between samples. Meanwhile, Inconel N06230 and Inconel 617 had lower tensile strength and overall variation.

Figure 8 shows the comparison of elongation values for various alloys. Various measurements (2-5 values in total) were taken for each metal at each flame condition.

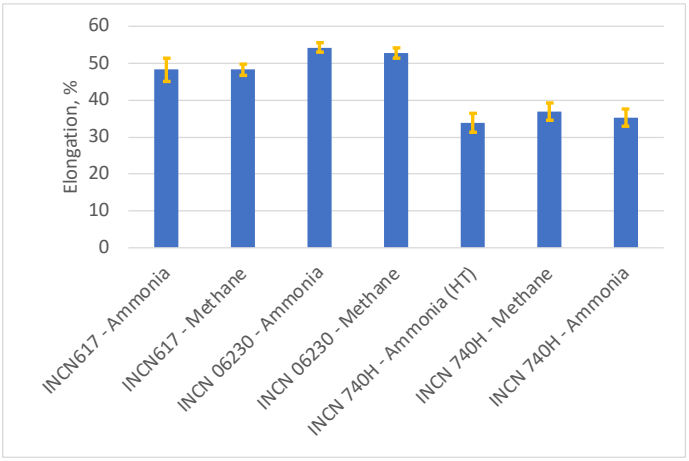

FIGURE 8: ELONGATION MEASUREMENTS FOR INCONEL617, INCONEL740H and INCONEL N06230

An F-test to check the equality of variances has shown that for all samples, the variances based on UTS are significantly different between the two flames. This is indicated by Figure 8 which shows a lower error bar for all methane measurements compared to ammonia/hydrogen flame measurements. Based on these preliminary findings, we can expect UTS and yield strength to be more precise indicators mechanical changes in the materials when compared to elongation, which is susceptible to larger sources of error from manual measurement and shows larger error for all flames and alloys. A paired t-test of unequal variances was conducted on the UTS values, at a 0.05 confidence level for each alloy. The results demonstrate that for all three alloys, there is insufficient evidence to show that there is a difference in the UTS of the methane flame exposed sample and the ammonia/hydrogen sample.

This is consistent with the fact that hydrogen embrittlement in superalloys has been reported when H>20-30 wppm [28], whereas the TDA results in the present work show much lower H levels. However, it must be noted that the measured H contents are for 5kW and were only exposed to ammonia/hydrogen flames for 5h; higher power and longer exposure times will most likely increase the H concentration within samples potentially reaching critical levels for embrittlement. Similarly, high-strength alloys, such as those with high γ' content, will adsorb more H due to their higher trapping capacity [26]. Further analyses need to be done to confirm whether hydrogen embrittlement in superalloys could happen under more extreme and realistic combustion conditions. For other metals, only the diffusible hydrogen is causing the embrittlement [31]. The lack of embrittlement found when testing at room temperature does not guarantee same mechanical properties in higher

temperatures. The presence of hydrogen that becomes diffusible above 300°C could still cause significant drop in properties while not being detectable in the room temperature.

Aside from metals, ceramic coatings are another important material selectively used in gas turbine combustors, for example platinum aluminide may be used for oxidation resistance on the turbine blades, while thermal barrier coatings may be used in the hottest sections of the combustion chamber [33]. To the author's best knowledge, most successful ammonia and ammonia/hydrogen gas turbine demonstrators have been focused on solving the combustion design challenges brought by these alternative fuels. As such, ammonia/hydrogen demonstrators have been manufactured from traditional metals (such as stainless steel) without coatings [34, 35].

Furthermore, most of the load in the combustor is carried through the core material and not the coating. Embrittlement in the core material could still cause failure and the coating is not expected to protect the metal from hydrogen diffusion at the surface. Some traditional coatings are vulnerable to hydrogen permeation and selection of new coatings for ammonia/hydrogen blends is expected to bring its own set of challenges and requires separate investigation.

4. CONCLUSION

- Nickel superalloys were exposed to premixed, swirl stabilised, methane and ammonia/hydrogen flames at 5 kW power for 5 hours.

- The alloys exposed to ammonia/hydrogen flames absorbed higher hydrogen content than methane exposed metals, which showed very little H contents. The hydrogen desorption/diffusion behaviour in samples exposed to ammonia/hydrogen flames is consistent with bulk diffusion and weak trapping, whereas deep trapping is likely taking place in the methane flames.

- Surface oxide layers were present in both combustion conditions showing different features, which are likely related to the oxidation/reduction process involved at the gas/metal interface. In addition, the oxide layer was shown to impact the hydrogen absorption and desorption rates by acting as deep traps against H diffusion.

- Although little effect in the loss of ductility was observed, due to the low temperatures and short exposure times, the combined results show that materials exposed to ammonia/hydrogen flames could be more prone to hydrogen embrittlement with high power combustion and longer exposure times. Hence, the results demand more in-depth investigations of H permeation and possible embrittlement in Nickel-based superalloys under realistic combustion conditions. Mechanical testing in elevated temperature could still show significant embrittlement.

ACKNOWLEDGEMENTS

The authors thank Special Metals Corporation for their generous donation of the samples used in this study and advise on the selection of metals suitable for ammonia/hydrogen combustion applications. This work was supported by funding from the EPSRC SAFE project (EP/T009314/1) and from project EP/T008687/2. The authors also thank Mr Malcolm Seaborne for his design and development of the combustion rig used in this study. E.I. Galindo-Nava acknowledges funding from RAEng for his research fellowship.

REFERENCES

[1] NH3 Fuel Association. 2019. "Introduction to NH3 Fuel." 2019. https://nh3fuelassociation.org/introduction/.

[2] Verkamp, F J, M C Hardin, and J R Williams. 1967. "Ammonia Combustion Properties and Performance in Gas-Turbine Burners." Proc. Combust. Inst. 11 (1): 985–92. https://doi.org/https://doi.org/10.1016/S0082-0784(67)80225-X.

[3] Pratt, D. T. 1967. "Performance of Ammonia-Fired Gas-Turbine Combustors." Defence Technical Information Centre.

[4] Gray, James T, Edward Dimitroff, Nelson T Meckel, and R D Quillian. 1967. "Ammonia Fuel — Engine Compatibility and Combustion." SAE Transactions 75 (October): 785–807. http://www.jstor.org/stable/44563675.

[5] Valera-Medina, A, H Xiao, M Owen-Jones, W I F David, and P J Bowen. 2018. "Ammonia for Power." Progress in Energy and Combustion Science 69: 63–102. https://doi.org/https://doi.org/10.1016/j.pecs.2018.07.001.

[6] Kobayashi, H, Hayakawa, A, K. D.Kunkuma A. S, and Ekenechukwu C. Okafor. 2019. "Science and Technology of Ammonia Combustion." Proc. Combust. Inst. 37 (1): 109–33. https://doi.org/10.1016/j.proci.2018.09.029.

[7] Brewster, Brandon S, Steven M Cannon, James R Farmer, and Fanli Meng. 1999. "Modeling of Lean Premixed Combustion in Stationary Gas Turbines." Progress in Energy and Combustion Science 25: 353–85.

[8] Joshi, N. D., Mongia, H. C., Leonard, G., Stegmaier, J. W., & Vickers, E. C. 1998. "Dry Low Emissions Combustor Development." In ASME 1998 International Gas Turbine and Aeroengine Congress and Exhibition. American Society of Mechanical Engineers.

[9] Valera-Medina, A, M Gutesa, H Xiao, D Pugh, A Giles, B Goktepe, R Marsh, and P Bowen. 2019. "Premixed Ammonia/Hydrogen Swirl Combustion under Rich Fuel Conditions for Gas Turbines Operation." International Journal of Hydrogen Energy 44 (16): 8615–26. https://doi.org/10.1016/j.ijhydene.2019.02.041.

[10] Starostin, M, A Grinberg Dana, O Dinner, G E Shter, and G S Grader. 2017. "High-Temperature Corrosion of Stainless Steels and Ni Alloys During Combustion of Urea–Ammonium Nitrate (UAN) Fuel." Oxidation of Metals 87 (1): 39–56. https://doi.org/10.1007/s11085-016-9655-7.

[11] Dana, A, M Starostin, G Shter, A Buk, Omry Dinner, and Gideon Grader. 2014. "Metal Corrosion Screening in a Nitrogen-Based Fuel at High Temperature and Pressure." Oxidation of Metals 82: 491–508. https://doi.org/10.1007/s11085-014-9504-5.

[12] Rezende, M C, L S Araujo, S B Gabriel, D S dos Santos, and L H de Almeida. 2015. "Hydrogen Embrittlement in Nickel-Based Superalloy 718: Relationship between Γ′ + Γ″ Precipitation and the Fracture Mode." International Journal of Hydrogen Energy 40 (47): 17075–83. https://doi.org/https://doi.org/10.1016/j.ijhydene.2015.07.053.

[13] Tarzimoghadam, Z, M Rohwerder, S.~V. Merzlikin, A Bashir, L Yedra, S Eswara, D Ponge, and D Raabe. 2016. "Multi-Scale and Spatially Resolved Hydrogen Mapping in a Ni-Nb Model Alloy Reveals the Role of the δ Phase in Hydrogen Embrittlement of Alloy 718." Acta Materialia 109 (May): 69–81. https://doi.org/10.1016/j.actamat.2016.02.053.

[14] Zhenbo Z, Moore K L, McMahon G, Morana R, and Preuss M,. 2019. "On the Role of Precipitates in Hydrogen Trapping and Hydrogen Embrittlement of a Nickel-Based Superalloy." Corrosion Science 146: 58–69. https://doi.org/https://doi.org/10.1016/j.corsci.2018.10.019.

[15] Verkamp, F. J.; Hardin, M. C.; Williams, J. R. "Ammonia Combustion Properties and Performance in Gas-Turbine Burners." Symp. Combust. 1967, 11 (1), 985–992. https://doi.org/https://doi.org/10.1016/S0082-0784(67)80225-X.

[16] Norton, D. G.; Vlachos, D. G. Combustion Characteristics and Flame Stability at the Microscale: A CFD Study of Premixed Methane/Air Mixtures. Chem. Eng. Sci. 2003, 58 (21), 4871–4882. https://doi.org/https://doi.org/10.1016/j.ces.2002.12.005.

[17] Saiki, Y., Fan, Y., Suzuki, Y. "Radical Quenching of Metal Wall Surface in a Methane-Air Premixed Flame" Combust. Flame 2015, 162, 4036–4045.

[18] Fan, Y., Guo, J., Lee, M., Iki, N., Suzuki, Y. 2021. "Quantitative Evaluation of Wall Chemical Effect in Hydrogen Flame Using Two-Photon Absorption LIF". Proc. Combust. Inst. 38 (2), 2361–2370. https://doi.org/https://doi.org/10.1016/j.proci.2020.06.021.

[19] Appari, S. Janardhanan, V. M., Jayanti, S., Maier, L., Tischer, S., Deutschmann, O. 2011. "Micro-Kinetic Modeling of NH_3 Decomposition on Ni and Its Application to Solid Oxide Fuel Cells." Chem. Eng. Sci., 66 (21), 5184–5191. https://doi.org/https://doi.org/10.1016/j.ces.2011.07.007.

[20] BSI Group. BS-EN-2032-001. Aerospace Series. Metallic Materials.; 2014.

[21] Vigueras-Zúñiga M, Tejeda-del-Cueto E M, Mashruk S, Kovaleva M, Ordóñez-Romero C L, and Valera-Medina A. 2021. "Methane/Ammonia Radical Formation during High Temperature Reactions in Swirl Burners." Energies 14 (20). https://doi.org/10.3390/en14206624.

[22] Gotama G J., Hayakawa A, Okafor E C., Kanoshima R, Hayashi M, Kudo T, and Kobayashi H. 2022. "Measurement of the Laminar Burning Velocity and Kinetics Study of the Importance of the Hydrogen Recovery Mechanism of Ammonia/Hydrogen/Air Premixed Flames." *Combustion and Flame* 236: 111753. https://doi.org/https://doi.org/10.1016/j.combustflame.2021.111753.

[23] Okafor, E C., Naito Y., Colson S., Ichikawa A., Kudo T., Hayakawa A., and Kobayashi H. 2019. "Measurement and Modelling of the Laminar Burning Velocity of Methane-Ammonia-Air Flames at High Pressures Using a Reduced Reaction Mechanism." Combustion and Flame 204: 162–75. https://doi.org/https://doi.org/10.1016/j.combustflame.2019.03.008.

[24] Quadakkers, W J, and J Żurek. 2010. "1.17 - Oxidation in Steam and Steam/Hydrogen Environments." In *Shreir's Corrosion*, edited by Bob Cottis, Michael Graham, Robert Lindsay, Stuart Lyon, Tony Richardson, David Scantlebury, and Howard Stott, 407–56. Oxford: Elsevier. https://doi.org/https://doi.org/10.1016/B978-044452787-5.00022-6.

[25] Symons D.M., Young G.A., Scully J.R.. 2001. "The effect of strain on the trapping of hydrogen at grain-boundary carbides in Ni-Cr-Fe alloys" Metallurgical and Materials Transactions A 32: 369-377

[26] Robertson W.M.. 1977. "Hydrogen permeation and diffusion in Inconel 718 and Incoloy 903" Metallurgical Transactions 8A: 1709-1712

[27] Titov A.A., Lun-Fu A.V., Gayvaronskiy A.V., Bubenchikov M.A., Bubenchikov A.M., Lider A.M., Syrtanov M.S., Kudiiarov V.N.. 2019. "Hydrogen accumulation and distribution in pipeline steel in intensified corrosion conditions", Metals 12: 1409

[28] Hicks P.D., Altstetter C.J.. 1992. “Hydrogen-enhanced cracking of superalloys”. Metallurgical Transactions 23A: 237-249

[29] Kharatyan S.L.,. Chatilyan H.A, Manukyan K.V.. 2019. “Kinetics and Mechanism of nickel oxide reduction by methane” The Journal of Physical Chemistry C 123: 21513-21521

[30] Ghali S., Eissa M., El-Faramawy H., Ahmed A, Baimoy F., Lamie M.. 2020. “Influence of Nitrogen on Oxidation Resistance of Automotive Steel Grades”. Key Engineering Materials 835: 83-92

[31] Takai K., Watanuki R., 2003 ‘Hydrogen in Trapping States Innocuous to Environmental Degradation of High-strength Steels’, ISIJ international, Vol. 43, issue 4, pp. 520-526

[32] Fry A., Osgerby S., Wright M., 2002 ‘Oxidation of Alloys in Steam Environments - A Review.’ NPL Rep. MATC(A)90

[33] Rajendran, R. Gas Turbine Coatings – An Overview. Eng. Fail. Anal. 2012, *26*, 355–369. https://doi.org/https://doi.org/10.1016/j.engfailanal.2012.07.007.

[34] Alboshmina, N. A. H. 2019. “Ammonia Cracking with Heat Transfer Improvement Technology.” PhD Thesis, Cardiff Un.

[35] Kurata O., Iki N., Matsunuma T., Inoue T., Tsujimura T., Furutani H., Kobayashi H., Hayakawa A., 2017 “Performances and emission characteristics of NH3–air and NH3CH4–air combustion gas-turbine power generations.” Proc. Combust. Inst. 36 3351–3359.